DOI: 10.1002/masy.200650911

Polymeric Multiporous Materials from Fibrillar Networks

*Debarshi Dasgupta, Arun K. Nandi**

Summary: Poly(vinylidene fluoride) (PVF_2) forms thermoreversible gels with liquid alkyl diesters as well as with camphor which is solid at room temperature. The diesters are replaced by another low boiling solvent cyclohexane by solvent exchange technique while camphor is dried just by exposing the material in vacuum to yield highly porous materials. Nano pores are generated as a result of solvent removal from polymer-solvent intercalates whereas macropores are contributed by percolation of polymer fibrils. The porosity thus created covers a wide range from 3 nm to 400 μm producing multiporous materials. Pores greater than 6 nm are measured by mercury intrusion porosimetry (MIP) and pores of diameter less than 6 nm is observed by N_2 adsorption porosimetry. The dried samples show two melting regions, low temperature hump for porous portion and high temperature peak for bulk portion. The porous materials have the ability to absorb water-soluble herbicides from around 10-ppm aqueous solution as indicated in UV spectrophotometric experiment.

Keywords: BJH isotherm; mercury intrusion porosimetry; multiporosity; polymer-solvent complex; thermoreversible gel

Introduction

Polymeric porous materials are systems of great interest in many industrial applications including biomedical, pharmaceutical, super absorbents and membranes. Fibrillar networks of polymers are obtained from thermoreversible gels of polymers. In case of crystalline polymers, fibrils are formed as a result of polymer-solvent complexation that inhibits the polymer chain folding process [1–3]. The polymer-solvent complexation is usually determined from thermodynamic, X-ray diffraction, neutron diffraction [4] and spectroscopic studies. A careful drying of the solvent from the polymer-solvent complexes may therefore give a network structure of polymer with meso and nano pores. Again thermoreversible gels are known to obey three-dimensional percolation model [2,5,6], though recently some controversy arises regarding the applicability of the model [7]. So the dried materials would also contain interconnected channel structure of macro dimensions. Thus a successful drying of a polymer gel without disturbing the gel structure would give rise to a multiporous material. Poly(vinylidene fluoride)(PVF_2) produces thermoreversible gels with different diesters of general formula $(CH_2)_n$ $(COOEt)_2$[1,2]. It also produces thermoreversible gel with camphor [3] (1,7,7-trimethyl bicyclo [2.2.1] heptane -2-one), which is solid at room temperature with strong sublimating tendency. Complexing PVF_2 with such a solid solvent is really a novel thought because the solvent can easily be removed from the gel just by applying high vacuum at room temperature to get the porous material. In this manuscript we shall deal with the porosity of dried PVF_2 -diethyl azelate (DEAZ) and PVF_2 – camphor gels.

Polymer Science Unit, Indian Association for the Cultivation of Science Jadavpur, Kolkata 700032, India
E-mail: psuakn@mahendra.iacs.res.in

Experimental

Samples

Poly (vinylidene fluoride) (PVF_2) is a product of Aldrich Chemical Co. Inc. The weight average molecular weight ($\overline{M}_w$) of the sample is 1,80,000 g/mole and polydispersity index is 2.54 as obtained from GPC. The PVF_2 sample was recrystallized from its 0.2% solution in acetophenone, washed with methanol and finally dried in vacuum at 60 °C for three days. The diester diethyl azelate (DEAZ) was purchased from Lancaster synthesis, Morecambe, England and were used as ?tlsb=0pt> received. D-L camphor was purchased from S. D. Fine Chemicals Ltd., Mumbai and was purified by sublimation procedure in vacuum at 50 °C. The herbicide Paraquat dichloride (PD) was received as a gift sample from Syngenta, Netherlands.

Porous Materials Preparation

PVF_2 and camphor were taken in a thick walled-glassed tube (8 mm in diameter and 1 mm thick) and were sealed. The sealed tubes were melted at 210 °C in an oven for 20 min with constant shaking to make homogeneous. The transparent melt was then quenched to room temperature (30 °C). The solid mass thus obtained was taken out from the tube and dried in vacuum at 40 °C for seven days. Complete removal of camphor was confirmed from the absence of >C=O stretching frequency (1740 cm^{-1}) in the FT IR spectrum of the samples. The PVF_2 -diethyl azelate gel were prepared in a sealed tube by melting the samples at 210 °C for 20 minutes and then quenched to 30 °C. They were then cut into pieces and dipped into cyclohexane for 4 days with occasional change of cyclohexane. It was finally replaced with methanol by dipping the gel in methanol for 1 day and dried at vacuum at 40 °C for 3 days.

Microscopy

For scanning electron microscopy (SEM) a thin film of PVF_2 camphor gel was melt casted and dried as above, gold coated with a gold layer of thickness 40 nm by the sputtering technique in an argon atmosphere and was observed in a SEM apparatus (Hitachi S-2300). The morphology of dried PVF_2 -diethyl azelate gel (PVF_2- DEAZ) was viewed in a field emission scanning electron microscope (FESEM) apparatus (JEOL, JSM-6700F) without any metal coating at accelerating voltage 1 kV.

Porosity Characterization

For porosity measurement both mercury intrusion porosimetry (MIP) and N_2 adsorption porosimetry were used. MIP was used to measure pores having diameter lying in the range 6 nm – 400 μm. For pores of diameter between 3–6 nm N_2 adsorption porosimetry was used. The MIP was done using the instrument Poremaster-33 (Quantachrome Instrument). The sample was first taken in a penetrometer (stem volume 2 cm^3) and inserted into the low-pressure station where mercury pressure was gradually increased from an initial 0.5 psi to 50 psi. Both intrusion and extrusion runs were recorded. The penetrometer was then taken out and some of the mercury was replaced by silicon oil and the entire system was then placed in the high-pressure station. In this station the pressure was increased to 33,000 psi then also both intrusion and extrusion runs were recorded. The data were analyzed by Porewin-32 software. The nitrogen adsorption porosimetry was done in SA 3100 surface area and pore size analyzer instrument (Beckman Coulter). BJH method was used to measure the pore diameter, using SA view software.

Thermal Characterization

The melting point and enthalpy of fusion of the dried gels were measured using a differential scanning calorimeter DSC-7 (Perkin Elmer) under N_2 atmosphere. The samples were heated from 50 °C to 230 °C at the rate 40 °C/min. The higher heating rate was chosen to avoid any melt recrystallization of the PVF_2 sample.[5]

UV-vis Spectroscopy

A 10-ppm aqueous solution of a herbicide, Paraquat dichloride (PD) is prepared in triple distilled water and the weighed amount of porous material was added to the known volume of that solution at concentration 0.15% (w/v). Then UV-vis spectra of the solution were taken in 1cm quartz cell from 190 nm to 1100 nm using a Hewlett-Packard spectrophotometer (model 8453) at 30 °C.

Result and Discussion

Morphology

Fig. 1(a) represents the surface structure of porous material obtained by removing camphor from PVF_2-camphor gel at weight fraction of PVF_2 ($W_{PVF2} = 0.20$). Pores of average pore size 3 μm are clearly seen in the micrograph. The morphology of the gel also depends on the polymer concentration [3]. Pores of nano dimensions (~20 nm) can be seen in some of the atomic force micrographs of this system.

Figure 1(b) represents the FESEM images of a dried gel obtained from PVF_2 -DEAZ (10% w/v). Fibrils of dimensions 25–30 nm and meso pores of different sizes (37–70 nm) are clearly observed in the micrograph. Existence of such thin fibrils supports the fact that solvent replacement technique is good enough to inhibit chain-collapsing phenomenon in PVF_2 gels of high boiling diesters during its drying [9].

Porosity

In Figure 2, high pressure and low-pressure mercury intrusion histograms are presented for dried PVF_2 -camphor gel ($W_{PVF2} =$ 0.20). Here intrusion volume normalized by sample weight is plotted against pore diameter. It is clear from the figure that a wide range of pore size distribution ranging from 10 nm to 400 μm exists in the sample. The material has high pore volume 3.56 cm^3/gm and high surface area 21.8 m^2/gm as obtained from MIP.

Here also multiscale pore size distribution is observed for both the high pressure and low pressure histograms. The former histogram shows pore sizes in the range 6 nm to 10 μm whereas the later shows pore distribution from 3 μm to 400 μm. Thus multiporous material is obtained in this system with porosity 1.81 cm^3/gm and surface area 96 m^2/gm. The meso pores are attributed to the polymer-solvent complex and the macropores are formed as a result of caging of solvent molecules between polymer fibrils.

In Figure 3, MIP histograms of cyclohexane dried PVF_2 - DEAZ (10% w/v) gel are presented.

In Figure 4(a) and 4(b) the hysteresis loops between mercury intrusion and extrusion processes of the above two samples are presented. It is apparent from each figure that there are interconnected channel type pores or ‘inkbottle’ pores present in the above materials. However, PVF_2 - DEAZ system has more hysteresis

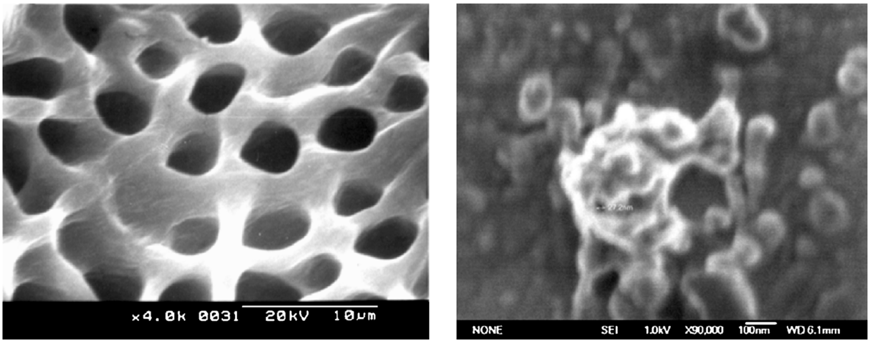

Figure 1.
left, Scanning electrom micrograph of dried PVF_2 -camphor gel ($W_{PVF2} = 0.20$). ***right*** Field Emission *scanning electron micrograph of dried PVF_2 -DEAZ gel* (10% w/v).

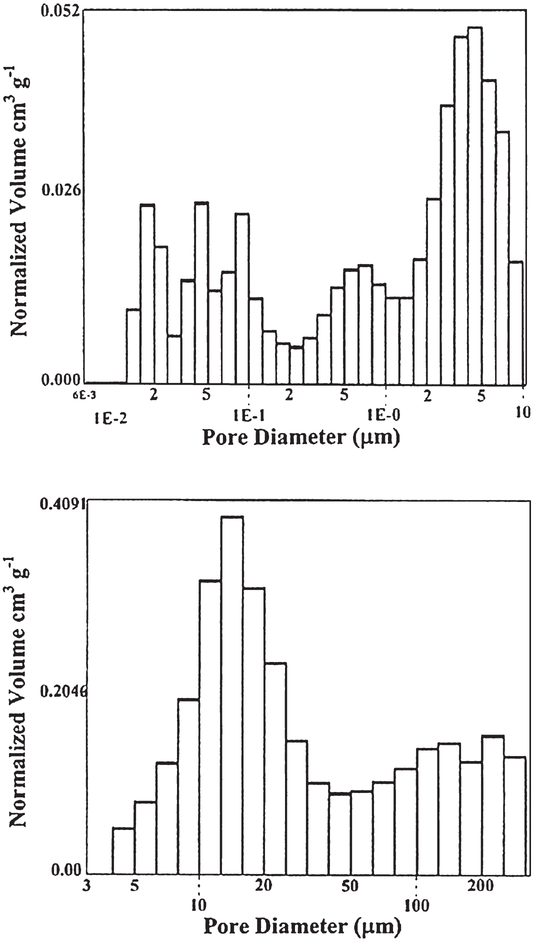

Figure 2.
MIP high and low-pressure histograms of dried PVF_2 camphor gel ($W_{PVF2} = 0.20$).

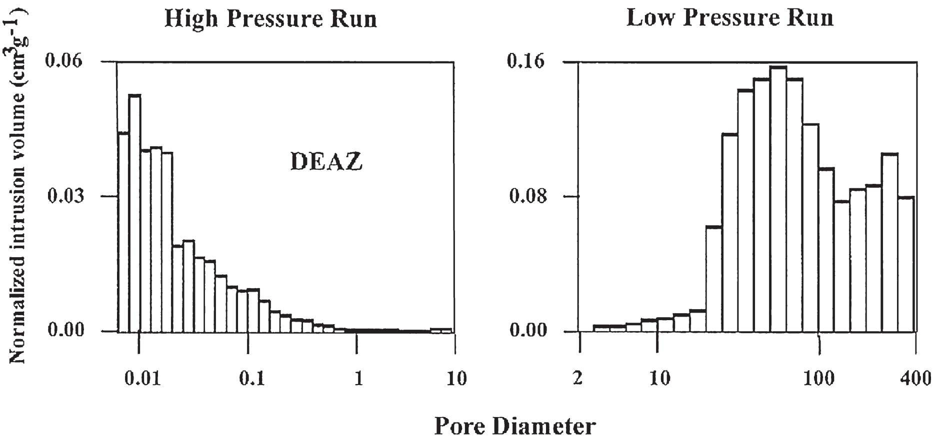

Figure 3.
MIP High-pressure and low pressure histograms of dried PVF_2 - DEAZ gel (10%w/v).

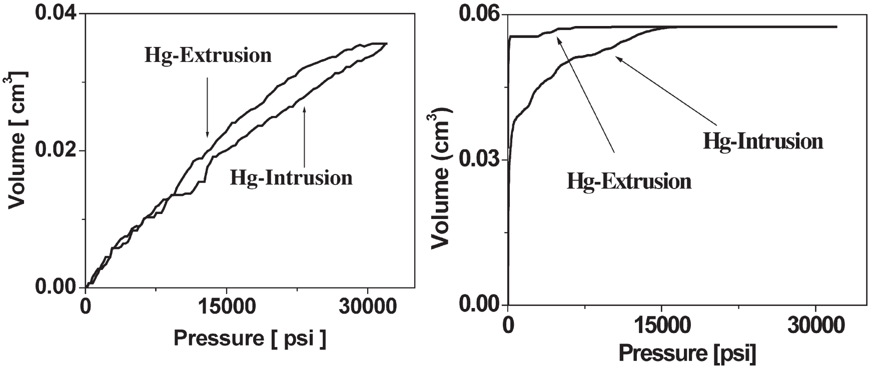

Figure 4.
left, Hysteresis loop of dried PVF_2 - DEAZ gel (10% w/v) and ***right*** Hysteresis loop of dried PVF_2 - camphor gel ($W_{PVF2} = 0.20$) obtained from MIP.

in the high-pressure range whereas PVF_2 - camphor system has prominent hysteresis in the low-pressure range.

These results clearly indicate that the interconnected channel type or 'inkbottle" type pores are more in mesoporous region of PVF_2-DEAZ system but it is larger in macroporous region of PVF_2 camphor system. In Figure 5(a) and 5(b) BJH pore volume distribution curves (desorption) of dried PVF_2-DEAZ gel (10% w/v) and dried PVF_2 -camphor ($W_{PVF2} = 0.1$) gel are presented. The maximum population of pores is obtained at a diameter 4.3 nm in the sample for the PVF_2 camphor system. In PVF_2-DEAZ, the minimum pore size observed is 3.6 nm and the maximum population of the pores is at 5.6 nm sizes.

It is noteworthy that due to limitation of the instrument we are unable to measure the pore sizes of diameter 1 nm which was depicted from MMX model.[9] However, pore size less than 3.6 nm can be depicted from the X-ray peaks of the sample (Figure 6) where peaks of d_{hkl} values 37, 25, 21 and 16 Å are clearly seen. This represents intercalation of three, two and one solvent molecules between the PVF_2 strands. The insets of Figure 5(a) and (b) represent the hysteresis loops of the respective samples. The lower curve is for adsorption process and the upper one is for desorption.

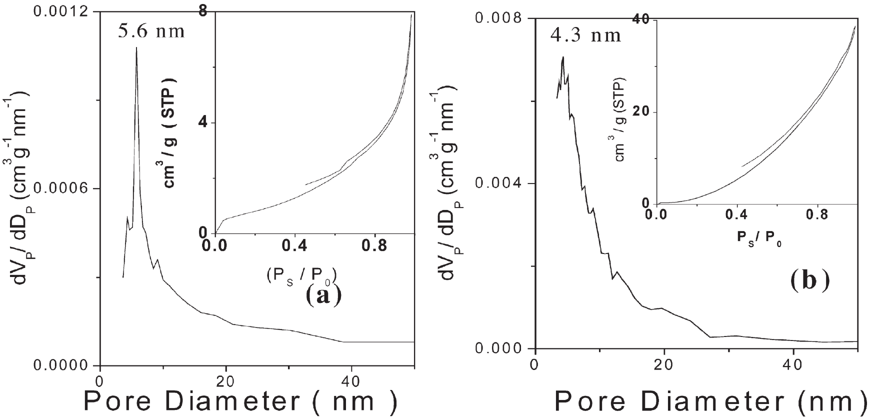

Figure 5.
left, BJH desorption pore volume distribution of dried PVF_2-DEAZ gel (10% w/v), ***right*** BJH desorption pore volume distribution of dried PVF_2-camphor gel (10% w/w) [Inset: Hysteresis loops between adsorption and desorption processes].

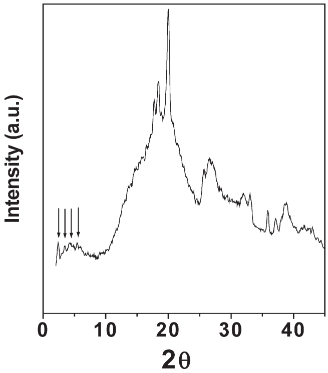

Figure 6.
WAXS pattern of dried PVF_2 DEAZ gel (10% w/v).

A distinct hysteresis can be observed in both the cases and this illustrates the 'ink-bottle' or interconnected channel like structure in the meso pores of both the systems. The micro and mesopores arise from the emptied calthrate formation in the PVF_2-camphor and PVF_2-DEAZ gels after solvent removal and the macropores in both the systems arise from the percolative structure of fibrillar networks.

Thermal Behavior

Figure 7(a, b) illustrates the DSC thermograms of dried PVF_2 - DEAZ and PVF_2-camphor gels at indicated weight fractions of PVF_2 at the heating rate 40°/min. In each figure each thermogram consists of a broad hump at lower temperature and an endothermic peak at higher temperature. The first elevation may correspond to the melting of the porous part of the material and the higher peak gives the melting information of the bulk part. This is because the crystalline domains in the porous part contain higher surface energy (as having high surface area) compared to that of the bulk part and the higher the surface energy the lower is the melting point [11]. The enthalpy of fusion values also increases with concentration. As for example in PVF_2-DEAZ system they are 60, 74 and 77 j/g for 10%, 15% and 25% (w/v) and for PVF_2-camphor system they are 54, 60, 59.5 and 59.3 j/g for 0.1, 0.25, 0.4 and 0.6 polymer weight fraction respectively. With increasing polymer concentration the fibrils become thicker and higher amount of heat is required to melt them so the enthalpy of fusion increase accordingly. This assertion can be supported from the melting point of bulk samples produced under melt-quenched condition.

This is shown in the Figure 8(a) and 8(b) for PVF_2 –DEAZ and PVF_2 –camphor

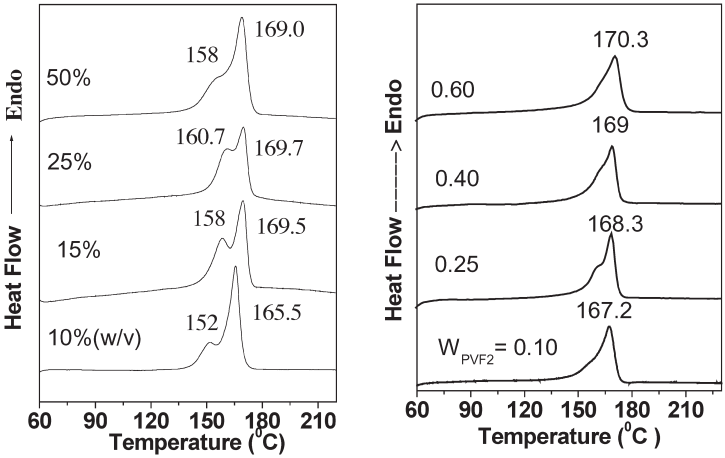

Figure 7.
left. DSC thermograms of dried PVF_2-DEAZ gel, ***right*** DSC thermograms of dried PVF_2-camphor gels at indicated weight fractions of PVF_2 at the heating rate 40°/min.

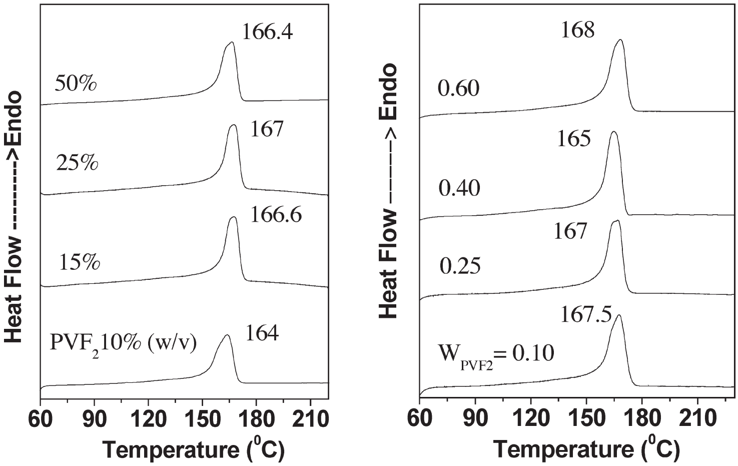

Figure 8.

left, DSC thermograms of melt-quenched PVF$_2$ from dried PVF$_2$-DEAZ gel, **right** DSC thermograms of melt-quenched PVF$_2$ from dried PVF$_2$-camphor gels in the melt quenched state at indicated weight fractions of PVF$_2$ at the heating rate 40°/min.

systems respectively. The melting temperature of the above samples in the melt-quenched sates are almost identical with each other with a single endothermic peak (Figure 8) at 167 °C Due to the thicker fibrils formation at increased polymer concentration the melting point of the melt-quenched PVF$_2$ is almost constant. Thus it may be concluded from the result that porous materials have lower melting point and it increases with increasing polymer concentration.

Sorption Behavior

Porous materials obtained from 0.2 weight fraction PVF$_2$ camphor gel adsorbs a potential water pollutant paraquat dichloride(PD), which is a herbicide from its 10-ppm solution. Figure 9 represents the UV-vis spectra of the 10-ppm stock solution of the pollutant PD (spectra a) and the same for solution of the pollutant after adding 0.15% (w/v) porous material of dried PVF$_2$-camphor gel (spectra b) to the solution The chemical structure of paraquat dichloride is given in the inset of Figure 9. The intensity of the characteristic peak of PD at 259 nm has decreased indicating that some of the pollutant is adsorbed by the porous material. Probably the pollutant enters into the nano pores and gets adsorbed and thereby the intensity of UV peak decreased by 20%. However such denomination of intensity is interesting as it concludes that 10-ppm paraquat dichloride may be removed completely by 0.75% (w/v) of porous material. More work is continued

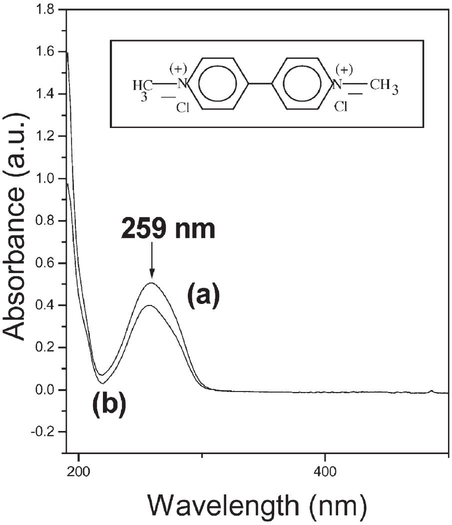

Figure 9.

UV-vis spectra of PD solution (a) before absorption and (b) after absorption by dried PVF$_2$ camphor (W$_{PVF2}$ = 0.2) **Inset:** Chemical structure of PD.

to decrease the pollutant content of different nature e.g. pesticides, herbicides, insecticides, small molecular organics and inorganic impurities (Hg, Pb, As, Fe salts) from wastewater.

Conclusion

It can be concluded that multiporous materials can be generated from PVF_2 thermoreversible gels. The materials have fibrillar network structure and they can be used as potential absorbent in separation technology.

Acknowledgement: We gratefully acknowledge IFCPAR grant No. 2808-2 for financial support of the work. We acknowledge Prof. J. M. Guenet of Institute Charles Sadron, Strasbourg, France for discussion. We are also grateful to Dr. Parag Bhargava and Dr. P. Pramanik of IIT-Kharagpur for their help in MIP and N_2 adsorption porosimetry measurement. Acknowledgement is also due to syngenta, Netherlands for their gift sample of herbicides.

[1] A. K. Dikshit, A. K. Nandi, *Macromolecules*, **2000**, 31, 2616.
[2] A. K. Dikshit, A. K. Nandi, *Macromolecules*, **1998**, 31, 8886.
[3] D. Dasgupta, S. Manna, S. Malik, C. Rochas, J. M. Guenet, A. K. Nandi, *Macromolecules*, **2005**, 38, 5602.
[4] S. Malik, C. Rochas, J. M. Guenet, *Macromolecules*, **2005**, 38(11), 4888.
[5] S. Mal, A. K. Nandi, *Polymer*, **1998**, 39, 6301.
[6] C. M. Chou, P. D. Hong, *Macromolecules*, **2003**, 36, 7331.
[7] J. M. Guenet, J. Rheol, *Macromolecules*, **2000**, 44, 947.
[8] W. M. Prest, Jr. D. J Luca, *J. Appl. Phys.* **1975**, 46, 4136.
[9] D. Dasgupta, A. K. Nandi, *Macromolecules*, **2005**, 38, 6504.
[10] H. Zhang, J. Sun, D. Ma, X. Bao, A. Klein-Hoffmann, G Weinberg, D. Su, R Schlogl, *J. Am. Chem. Soc.* **2004**, *126*, 7440.
[11] L. Mandelkern, In *Comprehensive Polymer Science*, Allen, G. Ed. Pargamon press, Oxford, **1989**, *vol-2*, page 363.